

Evolutionary Fields Can Explain Patterns of High Dimensional Complexity in Ecology

James Wilsenach*

*School of Informatics, Forrest Hill, University of Edinburgh,
5 Forest Road, EH1 2QL, Edinburgh, United Kingdom*

Pietro Landi† and Cang Hui‡

*Centre for Invasion Biology, Department of Mathematical Sciences,
Stellenbosch University, Private Bag X1, 7602, Matieland, South Africa*

(Dated: November 1, 2016)

One of the properties that make ecological systems so unique is the range of complex behavioural patterns that can be exhibited by even the simplest communities with only a few species. Much of this complexity is commonly attributed to stochastic factors which have very high-degrees of freedom. Orthodox study of the evolution of these simple networks has generally been limited in its ability to explain complexity, since it restricts evolutionary adaptation to an inertia-free process with few degrees of freedom in which only gradual, moderately complex behaviours are possible. We propose a model inspired by particle mediated field phenomena in classical physics in combination with fundamental concepts in adaptation, that suggests that small but high-dimensional chaotic dynamics near to the adaptive trait optimum could help explain complex properties shared by most ecological datasets, such as aperiodicity and pink, fractal noise spectra. By examining a simple predator-prey model and appealing to real ecological data, we show that this type of complexity could be easily confused for or confounded by stochasticity, especially when spurred on or amplified by stochastic factors that share variational and spectral properties with the underlying dynamics.

PACS numbers: 87.23.Kg, 87.23.Cc, 87.10.Ed

I. INTRODUCTION

Complexity in ecological data is characterized by long and short-term variations in behaviour across a wide range of time-scales, from generations to speciations, which are often difficult to predict. These erratic oscillations are commonly attributed to a combination of density-dependent, demographic and environmental stochastic factors, including variation caused by human intervention [1]. However, high-dimensional deterministic effects can be difficult to distinguish from high or infinite dimensional stochasticity, especially when data sets are relatively small (as is common in ecology). These patterns of variation have characteristic spectral compositions [2] and are often fractal in nature [3]. Field-based models of systems with many constituent particles have been used to understand many of the unpredictable and fractal systems found in physics [4–6], and were central to the development of complex systems research [7]. We ask whether a field, mediated by interacting individuals in evolving populations, could adequately describe some of the properties of ecological systems seen in nature by qualitative analysis of the field-based system as a whole and at the population level.

Dercole et al. [8] were the first to demonstrate a minimal adaptive ecological network, comprising three co-evolving species, prey, predator and super-predator, in

which red queen dynamical chaos in the co-evolution of traits leads to an increase in complex behaviour at the population level. However, slower, first order evolutionary dynamics constrain the complexity, period and magnitude of such chaotic oscillations. This results in part from fundamental properties of the so-called canonical equation in adaptive dynamics (AD) which admit only first order solutions in trait space [9, 10], thereby underspecifying some of the variability in ecological time series which is due to adaptation. In so doing, classical AD does not address the connection between the rate of adaptation and an organism's evolutionary trajectory, which is analogous to the relationship between velocity and momentum in physics, and which has been well supported by evolutionary theorists [11]. The evolutionary field formulation represents a higher order approach to trait adaptation, which can describe much of this complexity in even the simplest predator-prey systems. It does this in purely adaptive terms through high-dimensional trait-based chaos, which can arise from even a few traits. Our proposition therefore calls into question the orthodoxy of simple, low dimensional trait dynamics to adequately capture complexity (beyond purely periodic dynamics) and apparently random variation in ecological networks.

If higher order, high-dimensional deterministic dynamics are responsible for a portion of the apparent stochasticity seen in ecology, then such dynamics should share key characteristics with the stochastic processes they are trying to explain. As much as 80% of the apparent stochasticity in ecology is ascribed to coloured noise processes. Stochastic noise processes and, in particular, coloured noise, share many important properties with chaotic dynamics, including finite correlation dimensions

* s1666320@sms.ed.ac.uk

† landi@sun.ac.za

‡ African Institute for Mathematical Sciences, Muizenberg 7945, South Africa; chui@sun.ac.za

[3] and even positive Lyapunov exponents in some cases [12]. Coloured noise is characterized in terms of its spectral properties; however, certain dynamical systems have spectra which are qualitatively similar to noise [13].

We show that selective field forces, acting at a distance in trait space, are enough to superficially mimic many of these stochastic properties as well as attain a level of complexity comparable to real ecological data in the case of a simple predator-prey system. In Sec. II we present a formal justification of the model framework and parameters, followed by (in Sec. III) an exploration of the field model's dynamic and fractal chaotic behaviour in the chaotic, transient and aperiodic regimes. Here, we look specifically at intra-specific competition because of its established role in triggering instabilities and chaotic dynamics in population models [14, 15] and its importance in the variability of population data [16]. In Sec. IV we use historical field data on *Oryctolagus cuniculus*, the European rabbit in Britain [17] and *Lynx Canadensis*, the Canadian lynx [18] to determine whether the model fits with the qualitative behaviour of ecological systems. This was further investigated and tested in Sec. V using methods based on spectral analysis and the prominence of pink noise in ecological data with concluding remarks and further recommendations in Sec. VI.

II. MODEL JUSTIFICATION AND FORMULATION

The model relies on density-dependence as the primary determinant of biological interaction frequency, both at the population and, by implication, at the evolutionary level. This mass action approach underpins classical and modern theories in physics (e.g. gravitational and solid state physics [19]) and population ecology (e.g. Lotka-Volterra and AD models [20]). The evolutionary field model extends these ideas into evolutionary ecology by considering each biotic interaction as an exchange of fitness information between populations. An understanding of the model relies on interpreting individuals interacting within and between species, as mediators of an evolutionary force which is translated to adaptive change in a generalized trait space (an abstract representation of multiple independent, continuous traits). The model is also partially motivated by recognising the role played by density-dependence in both stochastic and dynamical complex behaviour in ecology (e.g. in inducing population level chaos in classical ecological models [21]). However, density considerations only describe the frequency, not the strength or type of individual interactions between members of two species. Both competitive and antagonistic interaction strengths have largely been measured in the past by trait matching, in which distances between individuals' traits have some bearing on the strength of their interaction. This is motivated by the assumption that trait matching translates into stronger, more direct competition and more efficient consumption,

or cooperation (in the case of mutualistic interactions). This does not mean that the two species are necessarily similar in phenotype as the traits relevant to each species in the interaction could differ in type or scale.

The functional form of the distance assumes an assortative selection force of the type used in other adaptive dynamics models [22–25], namely a power law measure of interaction strength based on the Euclidean norm ($\|\cdot\|$), where a smaller euclidean distance between traits implies stronger trait matching. Power law distance (d_{ij}) and direction (\mathbf{u}_{ij}) inform the assumed topology of the trait space, with trait vector $\mathbf{a}_i = (x_i, y_i) \in \mathbb{R}^2$ for species i ; they are defined as:

$$d_{ij} = e^{\|\mathbf{a}_i - \mathbf{a}_j\|^2} \quad \mathbf{u}_{ij} = \frac{\mathbf{a}_j - \mathbf{a}_i}{\|\mathbf{a}_j - \mathbf{a}_i\|} \quad (1)$$

By combining the role of mass action, in mediating population interaction frequency, assortative selection, in determining interaction strength and selective action, between organisms operating at a distance in trait space (see Eq. (1)), we can define a set of second order evolutionary field equations which govern the dynamics of the trait vector $\mathbf{a}_i = (x_i, y_i)$ for species i with population mass m_i as defined by:

$$\frac{d^2 \mathbf{a}_i}{d\tau^2} = \theta_i \left[\sum_{j=1}^N k_{ij} \frac{m_i m_j}{d_{ij}} \mathbf{u}_{ij} - f \frac{d\mathbf{a}_i}{d\tau} \left| \frac{d\mathbf{a}_i}{d\tau} \right| \right] \quad (2)$$

Here $\theta_i = \mu_i m_i$, gives the population mutation rate from individual mutation rate, μ_i , and f represents the coefficient of the resistance in the population to rapid changes in adaptation rate. This f term is based on an analogy with fluid drag under the assumption of finite gene flow within a population that also takes into account limitations on adaptation through physiological restrictions on generation time. The combination of the k_{ij} and k_{ji} interaction coefficients define the type (mutualistic, predatory, competitive etc.) and maximum potential interaction strength between species i and j . These types are characterised by the effect that interaction with members of species j usually has on the fitness and abundance of members of species i and can be either antagonistic ($k_{ij} < 0$) or beneficial ($k_{ij} > 0$). Interactions resulting in changes at the population level translate into slower changes at the adaptive level through repulsive ($k_{ij} < 0$) or attractive ($k_{ij} > 0$) field effects on species i with respect to j in trait space. These k_{ij} factors determine the maximum potential interaction because of the bound imposed by the electrostatic or gravity-like inverse (exponential) squared law given by the d_{ij}^{-1} factor in Eq. (2). Since there are no constraints on the signs of the k_{ij} and k_{ji} pairs, this allows for the set up of pseudo-gravitational adaptive competitions between i and j , which permit masses (population masses in our biological context) of different signs, but otherwise behave the same way as electrostatic (or gravitational) attraction or repulsion [26]. In general $k_{ii} < 0$ and represents

the negative relationship between population density and the availability of environmental resources such as territory.

The population mass dynamics for the prey, m_1 , and predator, m_2 , are then defined by:

$$\frac{dm_1}{dt} = \left[r_1 + k_{11}m_1 + \frac{k_{12}}{d_{12}}m_2 + \frac{k_{1s}}{d_{1s}}m_s \right] m_1 \quad (3)$$

$$\frac{dm_2}{dt} = \left[r_2 + k_{22}m_2 + \frac{k_{21}}{d_{21}}m_1 \right] m_2 \quad (4)$$

(See Eq. (A.1) and (A.2) for parametrisation.) Here class s represents the stationary resource which, for simplicity, can be considered a density-independent environmental resource or to be sufficiently abundant to be unaffected by prey consumption (i.e. it has a fixed density of $m_s = 1$). It is also non-adaptive, existing at a fixed position at the origin in trait space (i.e. $\mathbf{a}_s = \mathbf{0}$). The model does not treat intraspecific competition, represented by k_{ii} (defined in Eq. (3) and (4)), or death rate r_i as adaptive and are thus independent of trait distance and matching. The two separate time scales τ and t are such that $T = \frac{d\tau}{dt} < 1$, but, since adaptation is assumed to occur according to a second order process, this means that T^2 is the time scale factor of relevance to the higher order dynamics.

III. DIMENSIONALITY AND CHAOS

FIG. 1 shows the results of simulation of a typical trajectory (after exclusion of 10^4 TU of transient) for the case where the relationship between prey and predator intraspecific competition (k_{ii}) is $k_{11} = 0.5 < k_{22} = 0.8$, with $1.1 = \mu_1 > \mu_2 = 1$. The system exhibits aperiodic cycling at the trait and population levels. Strong positive correlation ($\rho_{XY} = 0.68$), evident between inter-species trait distance and prey abundance, indicates that an assortative force generated by a pseudo-gravitational field can lead to population fluctuations closely linked to co-evolutionary change.

The correlation dimension, D_2 , is an established measure of the fractal dimension of chaotic attractors [27] which is defined in terms of the distribution of randomly sampled points on the attractor. Calculating the correlation dimension, D_2 , requires the computation of the correlation integral which can be approximated with real or simulated time series of size N by the correlation sum $C(r)$. The correlation sum [28] is a weighted count of points from the series within a given radius r , of each other.

$$C(r) = \frac{2}{(N-c)(N-1-c)} \sum_{i=1}^N \sum_{j=1}^{i-c} H(r - \|\mathbf{x}_i - \mathbf{x}_j\|)$$

Here $H(x)$ is the Heaviside step function, $\|\cdot\|$ is the Euclidean norm and \mathbf{x}_i are time-indexed points from a multidimensional time series. The integer c defines a correlation length, and is used to exclude values that are close

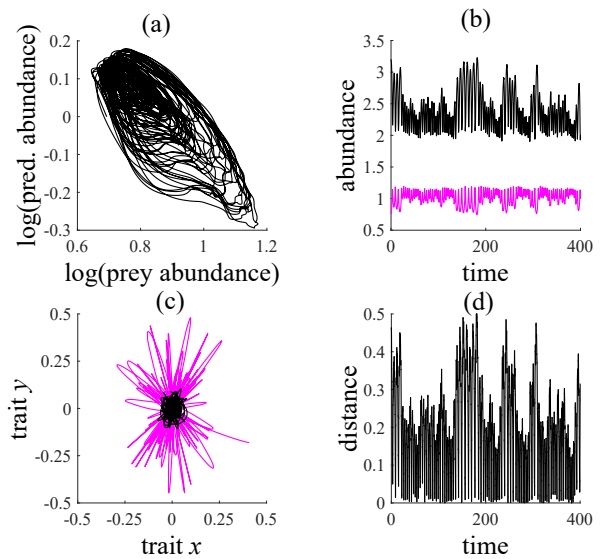


FIG. 1. (Colour Online) Aperiodic predator-prey system behaviour at both the trait and population levels plotted for 400 time units (TU) in the case where prey intraspecific competition, $k_{11} = 0.5$. (a.) Log abundance-abundance and (b.) abundance-time for prey (m_1) and predator (m_2). (c.) Prey (\mathbf{a}_1) and predator (\mathbf{a}_2) trait space dynamics in a 2D trait space that shows aperiodic orbiting of the fitness optimum. (d.) Euclidean distance ($\|\mathbf{a}_1 - \mathbf{a}_2\|$) between predator and prey in trait space with stationary exhibiting aperiodic behaviour.

neighbours in time. The following relationship holds between the fractal dimension D_2 , the radius r and the correlation sum, $C(r)$:

$$C(r) \propto r^{D_2} \quad (5)$$

Due to this power law D_2 is approximated by the slope of the scaling region of the log-log plot of $C(r)$ versus r . From FIG. 2 this gives an estimate of $D_2 \approx 5.7$ for the correlation dimension of the attractor. D_2 depends on the choice of scaling region and the value of parameters. For different values of the k_{ij} interaction coefficients D_2 takes on a value $D_2 \in [2.1, 6.3]$ for prey intraspecific competition $k_{11} \in [0.4, 0.7]$ and $D_2 \approx 2.1$ for $k_{11} \in [0.8, 0.9]$.

The presence of dynamical chaos in a time series can be detected using Wolf's algorithm [29]. This algorithm uses the defining feature of chaos, exponential-time orbital divergence under small perturbations, to determine the largest Lyapunov exponent, λ_1 . In order to show that dynamical chaos can be recovered from a variable more likely to be observed in the field, phase space reconstruction was carried out using prey abundance (m_1). The reconstruction was performed using the time-delay embedding theorem of Takens [30]. An embedding dimension of 6 was chosen by taking the ceiling of the previous result for the correlation dimension and the time-delay was approximated using the first minimum of the auto-mutual information according to the method of Fraser and Swinney [31] (FIG. 3a). Investigation of λ_1 for a range of

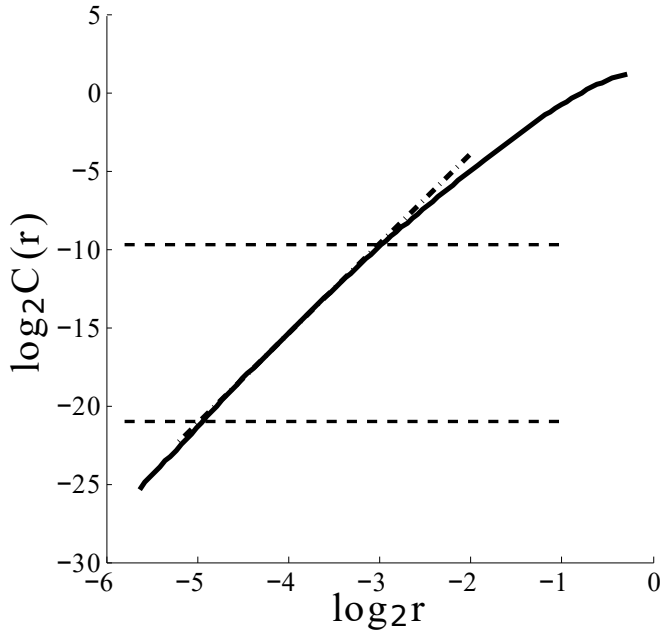


FIG. 2. Log-Log plot of the correlation sum as a function of radius when prey density, $k_{11} = 0.5$. Horizontal, dashed lines indicate the bounds of the scaling region, where the log sum is near linear (in accordance with Eq. (5)) with slope $\hat{D}_2 = 5.7 \pm 0.1$ (linear fit given by dashed line).

parametrisations of prey density-dependence, k_{11} , shows a change in behaviour for $k_{11} \geq k_c \approx k_{22} = 0.8$ (k_{22} is the coefficient of predator intraspecific competition) from a positive to negligible (possibly non-positive) λ_1 value, indicative of a bifurcation to chaos. This demonstrates a potential route to chaos for this predator-prey system dependent on the relationship between predator and prey density. The role of density-dependence in ecological chaos and in population stability and robustness has been widely supported in theory and simulation [14, 15, 21]. This behaviour may also represent an adaptive form of the Paradox of Enrichment presented in a highly controversial and influential paper by Rosenzweig [32] in which de-stabilization of both populations can result from lowering the resource restrictions on prey. Transient chaotic behaviour can result from the creation of an unstable chaotic manifold through the crisis (periodic) or the crisis-like (quasi-periodic) route to chaos [33]. Steady state dynamics following chaotic transients can be periodic, quasi-periodic or even include chaotic behaviour on a secondary attractor. Transient behaviour can be relatively persistent and can remain even after far exceeding the bifurcation value k_c [34]. In addition the steady state can be sensitive to any perturbations which could cause the system to re-enter a potentially long chaotic transient again [35]. The behaviour of the two species system for $k_{11} \geq k_c$ seems to exhibit such chaotic transient behaviour with a quasi-periodic steady state (FIG. 4). The combination of even the lowest levels of noise and the presence of a chaotic repeller for $k_{11} > k_c$

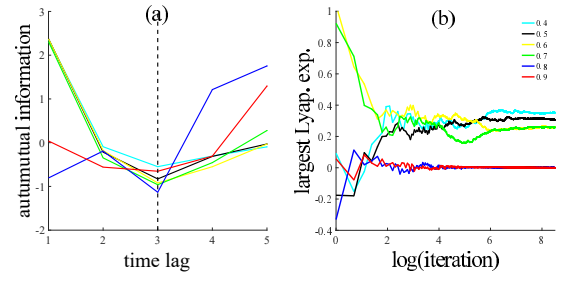


FIG. 3. (Colour Online) (a.) Normalized, time-lagged mutual information (in bits, legend given in (b.)) for the prey population time series (m_1). The dotted line shows the first minimum (and thus the proposed delay time) as 3. (b.) Estimate of the Largest Lyapunov exponent (λ_1) estimated by the Wolf algorithm as the number of iterations (on a log scale) increases. The legend shows the parametrisations of prey intraspecific competition (k_{11}) between 0.4 and 0.9.

could lead a simple predator-prey system to persist in a chaotic state.

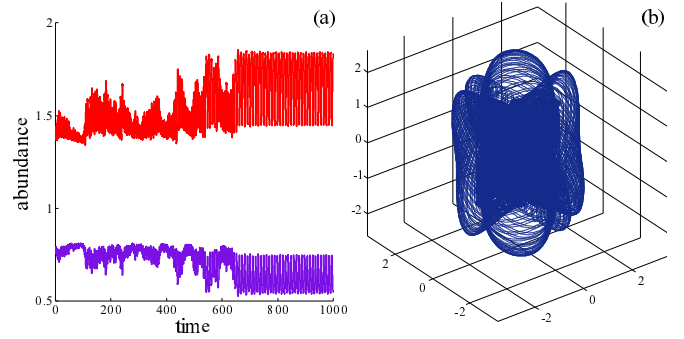


FIG. 4. (Colour Online) (a.) Transient chaotic behaviour in species abundance when prey intraspecific competition, (k_{11}) is 0.9, showing prey (m_1 - red as in FIG. 3) and predator (m_2 - purple) time series. (b.) Time-delay reconstruction of a prey trait (x_1) time series (after transient), embedded in three dimensional space, exhibiting high-dimensional, non-chaotic (quasi-periodic) behaviour.

IV. MODEL FIT TO PREY SPECIES DATA

Ecological time series were obtained from work by Middleton on the European rabbit *Oryctolagus cuniculus*, gathered annually in Norfolk (site B), Eastern lowland Britain, from 1862 to 1932 [17]. The European rabbit has been shown to dominate the diet of lowland red foxes (*Vulpes vulpes*) in all seasons. The rabbit constitutes 74% of mass ingested annually [36]. FIG. 5 shows the results of fitting the model using a loose minimum squared error (SE) approach, on 10^4 data points (not including transient) of the simulated prey abundance. The time series were generated using the parametrisations already explored. The model was fitted to the data by sampling at

different rates from the model (with a period of between 5TU and 70TU) using a moving window of the same size as the data set. The least-squares error was then calculated across all such windows and values of prey density dependence (k_{11} from 0.4 to 0.9) to obtain the best fit for the data.

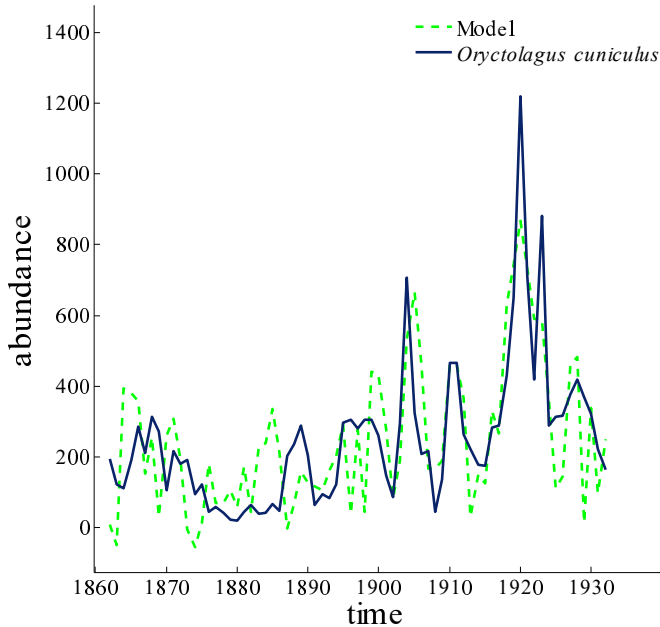


FIG. 5. (Colour Online) Model fit (dotted - green, as in FIG. 3) to Middleton, *Oryctolagus cuniculus*, data (solid) from Norfolk B, 1932-1862, using a fitted prey intraspecific competition coefficient (k_{11}) of 0.7 and a fitted sampling period of 7TU. These parameters were selected by windowed least squares fitting from simulated time series.

V. NOISE GENERATION AND SPECTRAL COMPARISON OF MODEL WITH DATA

Pink noise describes a family of random signals termed coloured noise which contaminate a vast range of real world signals, including the majority of ecological time series data [2, 37, 38]. The presence of pink noise is characterised by long-term correlations in the series. It is defined by the inverse relationship between the frequencies present in the underlying signal $x(t)$ of the time series and the amount of energy (variation) present at each frequency, known as the power spectral density, (PSD) of the signal at f , denoted $S_{xx}(f)$. The relationship can be expressed as

$$S_{xx}(f) \propto \frac{1}{f^\alpha} \quad (6)$$

where $0 \leq \alpha < 3$ is the noise scaling exponent which determines the rate at which power drops off with frequency. Typically, any signal for which $2 > \alpha > 0$ is said to be reddened, while noise where $\alpha \approx 1$ is known

as pink noise. In contrast, white noise is a random signal with a constant power level over all frequencies i.e. $S_{xx}(f) \propto 1$. A property that distinguishes pink from white noise and which makes pink noise even more interesting from a dynamical perspective is that pink noise possesses finite fractal dimension dependent on the value of α . This makes it more difficult to distinguish from the underlying dynamics with the use of fractal analysis [3]. This relationship is restricted to $1 < \alpha < 3$.

$$D_2(\alpha) = \frac{2}{\alpha - 1}$$

A method for estimation of the α noise exponent, $\hat{\alpha}$, in short, stationary ecological time series was followed, as presented by Miramontes and Rohani [39]. This method has been used effectively to identify exponents in series as short as 40 data points [37]. The standard method utilizes the direct estimation of PSD via the absolute square of the Fourier Series. However, a more accurate method for PSD estimation was used here, the so-called Multitaper approach proposed by Thomson [40]. The Multitaper method is a non-parametric method of PSD estimation which reconstructs the spectrum by averaging over pairwise-orthogonal windowed segments of the original series (which are thus statistically independent). This method has a number of advantages over the direct Fourier transform in that it is not dominated by bias, and the averaging of orthogonal data windows has the effect of smoothing out some of the noise caused by sample size limitations. The value of $\hat{\alpha}$ for the Middleton data was calculated as 0.948 with a 95% confidence interval of $CI = [0.383, 1.51]$. In comparison, for the fitted data $\hat{\alpha} = 1.13 \in CI$. This suggests agreement at the spectral level, not just between the model and data, but also with previous results for long ecological series. Spectral similarities persist for longer, chaotic time series as well.

Simulated pink noise data was generated using the digital signal generation method produced by Kasdin, and also independently by Hoskings [41, 42], which relies on convolution of a white noise series with a transfer function. In FIG. 6, negative linear trend dominates in the log-log PSD plots for all chaotic intraspecific competition (k_{11}) parametrisations. The chaotic signals mimic the simulated pink noise data in their qualitative behaviour (with comparable trend and slope) at all but the lowest frequencies where higher variation is present in the pink series, however, this discrepancy may become difficult to notice in short ecological series. The shared negative linear trend and slope in the higher frequency log spectrum indicates a shared power law variance drop-off relationship (see Eq. (6)) between the chaotic model and noise signals.

A non-parametric method to distinguish chaos from a series generated by any coloured noise process has been proposed by Kennel and Isabel, which uses a Kolmogorov-Smirnov statistic derived from simulating the prediction error of a large number of surrogate data. The surrogate data are based on the original query series with

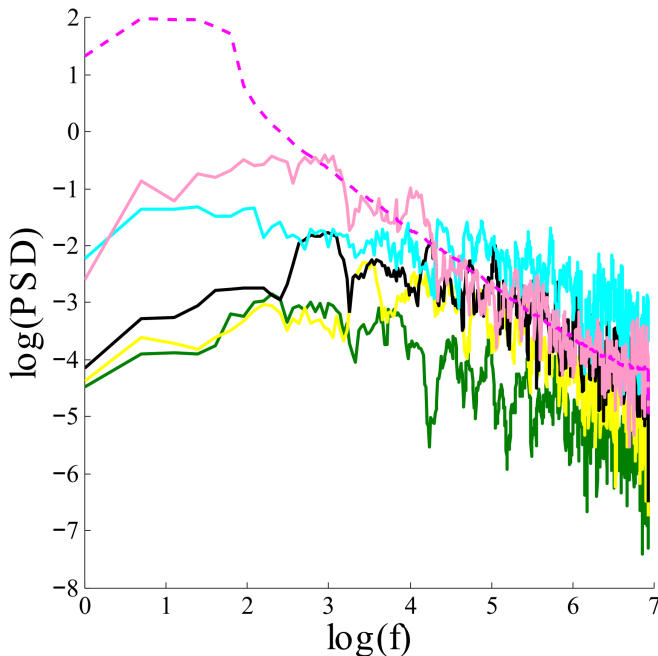


FIG. 6. (Colour Online) Log-log spectral density (variance in each frequency) reconstructed from simulated prey population series (m_1 - colour as in FIG. 3) at a sampling period of 7/TU (totalling 1429 data points per parametrisation), determined by estimation from Middleton data. Includes spectra from pink noise that has been smoothed (dotted magenta), by averaging 1000 individual signals, and a single representative realization (solid pink), both with the same total variance as the model time series with intraspecific competition (k_{11}) equal to 0.5. Superficially similar decreasing linear trend between pink and chaotic spectra indicates variational similarities.

Gaussian noise added in the frequency domain [43]. The Kolmogorov-Smirnov statistic should behave as a standard normal random variable under the null hypothesis of no difference in generating distribution. Using a prediction step size of one, this method fails to distinguish our fitted model time series from coloured noise using a two-sided z-test ($z = -0.084 > z_{0.05}$). This is in comparison with a value of $z = -0.307 > z_{0.05}$ for the *Oryctolagus cuniculus* field data. Importantly, it can be shown that certain ecological time series of predator-prey systems have compositions significantly different from noise at the 99% confidence level, suggesting that other processes (e.g. periodic or quasiperiodic dynamics) dominate the spectrum. Data obtained from historical fur sales records of the Canadian lynx, *Lynx canadensis*, in the MacKenzie River area of Canada, were obtained for the years 1821 to 1934 [18]. The test statistic calculated for these data was $z = -2.86 < z_{0.005}$. This result means that, despite data size limitations, the test has sufficient power to detect significant deviations from coloured noise in some cases. Interestingly, fitting of the Canadian lynx data by the same process as used for the Middleton data, gives a non-chaotic parametrisation of best fit with in-

traspecific competition, $k_{11} = 0.8$ (in the quasiperiodic region). This demonstrates the versatility of adaptive models to explain different kinds of variation in data.

VI. DISCUSSION

We have presented an eco-evolutionary model inspired by field ideas in physics which, using sufficiently fast evolving traits (such as behavioural adaptations to predation), can explain complex patterns of population variability seen in simple ecological systems. The model is able to account not only for qualitative behaviour within specific ecological time series (*Oryctolagus cuniculus*) but shows that high-dimensional adaptive models can have variational distributions characteristic of ecological systems in general. This characteristic red shift seen in the spectral composition of our model is consistent with prior results for the majority of ecological time series and moreover shows that such properties need not arise from purely stochastic processes in ecology. Our findings do not supersede stochastic explanations but do show how high-dimensional, deterministic ecological dynamics (based on second order adaptive dynamics) and environmental stochasticity could sustain and reinforce each other leading to the complex variational patterns found in ecology.

The role played by intraspecific competition in triggering a bifurcation to dynamical chaos is also notable in that it is in agreement with previous theoretical and observational research on the relationship between stability, variability and density dependence [14, 15, 21]. It also shows an alternative route to an effect similar to the paradox of enrichment [32], since decreased strain on the prey population leads to population instability in the prey and the system as a whole.

Although evolutionary field theory represents a different approach to classical adaptive dynamics, the principle that ecological models demand greater capacity for complexity than has currently been achieved is evident. The potential for field thinking in ecology may represent an underlying mechanical symmetry between ecology and physics and provide a new conceptual source for classical, game-theoretic models. Such models could be more easily extended to higher dimensional systems including those with multiple, species and traits, with less fine tuning than is generally required from current adaptive dynamics approaches.

ACKNOWLEDGMENTS

This research was first presented as part of a BSc (Hons) thesis at the University of Stellenbosch with helpful advice from members of Stellenbosch University's Mathematics Department, notably Farai Nyabadza, the African Institute for Mathematical Sciences (AIMS), notably Jeff Sanders and Zoe Wyatt and the South

African Centre for Epidemiological Modelling and Analysis (SACEMA), notably Brian Williams. The research was funded by the National Research Foundation (NRF) of South Africa through the South African Research Chair Initiative and the Competitive Program for Rated Researchers (NRF grants 81825 and 76912) with additional backing from SACEMA and AIMS.

Appendix: Parametrization

The full model parametrisation is presented here in a matrix format similar to the Lotka-Volterra models on

which the population component is based.

$$k_{ij} = \begin{pmatrix} 1 & 2 & s \\ \star & -1 & 2 \\ 0.5 & -0.8 & 0 \\ 0 & 0 & 0 \end{pmatrix} \begin{matrix} 1 \\ 2 \\ s \end{matrix} \quad r_i = \begin{pmatrix} -0.002 \\ -0.003 \end{pmatrix} \begin{matrix} 1 \\ 2 \end{matrix} \quad (\text{A.1})$$

$$\mu_i = \begin{pmatrix} 1.1 \\ 1 \end{pmatrix} \begin{matrix} 1 \\ 2 \end{matrix} \quad T = 0.5 \quad f = 1 \quad (\text{A.2})$$

The \star for k_{11} is a place holder that denotes the changing value of prey density-dependence (k_{11}) between sections and figures. These values are (in order of appearance).

$$k_{11} \in \{0.5, 0.4, 0.5, 0.6, 0.7, 0.8, 0.9\} \quad (\text{A.3})$$

(Colour Online) Where the text colour of parameter values correspond with the plotted colour for figures relating to prey abundance (m_1) simulations. Other colours are specified when considering other system variables for a specific value of the density-dependence (k_{11}).

-
- [1] O. Bjørnstad and B. Grenfell, *Science* **293**, 638 (2001).
 - [2] S. Pimm and A. Redfearn, *Nature (London)* **334**, 613 (1988).
 - [3] A. Osborne and A. Provenzale, *Physica D* **35**, 357 (1989).
 - [4] J. Hietarinta and S. Mikkola, *Chaos* **3**, 183 (1993).
 - [5] S. Goldfain, *Chaos, Solitons & Fractals* **28**, 913 (2006).
 - [6] L. Nottale, *Chaos Solitons Fractals* **7**, 877 (1996).
 - [7] M. Gutzwiller, *Rev. Mod. Phys.* **70**, 589 (1998).
 - [8] R. F. F. Dercole and S. Rinaldi, *Proc. R. Soc. B.* **277**, 2321 (2010).
 - [9] U. Dieckmann and R. Law, *J. Math. Biol.* **34**, 579 (1996).
 - [10] G. M. F. J. J. V. H. J. Metz, S. Geritz, (1996).
 - [11] G. Simpson, *Tempo and mode in evolution*, 15 (Columbia University Press, 1944).
 - [12] M. Dämmig and F. Mitschke, *Phys. Lett. A* **178**, 385 (1993).
 - [13] P. Manneville, *J. Phys. (Paris)* **41**, 1235 (1980).
 - [14] R. May, *Science* **186**, 645 (1974).
 - [15] R. May, *Nature (London)* **261**, 459 (1976).
 - [16] I. Hanski, *Phil. Trans. R. Soc. B* **330**, 141 (1990).
 - [17] A. Middleton, *J. Anim. Ecol.* , 231 (1934).
 - [18] C. Elton and M. Nicholson, *J. of Anim. Ecol.* , 215 (1942).
 - [19] H. Y. N. G. A. J. G. A. J. Y. D. M. D. X. J.S. Ross, S. Wu and W. Yao, *Nat. Commun.* **4**, 1474 (2013).
 - [20] F. Dercole, *Theor. Ecol.* , 1 (2015).
 - [21] A. Berryman and J. Millstein, *Trends Ecol. Evol.* **4**, 26 (1989).
 - [22] A. Rossberg, Å. Brännström, and U. Dieckmann, *Theor. Ecol.* **3**, 13 (2010).
 - [23] F. S. Valdovinos, R. Ramos-Jiliberto, L. Garay-Narváez, P. Urbani, and J. A. Dunne, *Ecol. Lett.* **13**, 1546 (2010).
 - [24] F. Zhang, C. Hui, and A. Pauw, *Evolution* **67**, 548 (2013).
 - [25] F. D. P. Landi and S. Rinaldi, *SIAM J. Appl. Math.* **73**, 1634 (2013).
 - [26] H. Bondi, *Rev. Mod. Phys.* **29**, 423 (1957).
 - [27] P. Grassberger and I. Procaccia, *Physica D* **9**, 189 (1983).
 - [28] J. Theiler, *Phys. Rev. A* **34**, 2427 (1986).
 - [29] H. S. A. Wolf, J.B. Swift and J. Vastano, *Physica D* **16**, 285 (1985).
 - [30] F. Takens, *Detecting strange attractors in turbulence* (Springer, 1981).
 - [31] A. Fraser and H. Swinney, *Phys. Rev. A* **33**, 1134 (1986).
 - [32] M. Rosenzweig, *Science* **171**, 385 (1971).
 - [33] E. O. C. Grebogi and J. Yorke, *Physica D* **7**, 181 (1983).
 - [34] E. O. C. Grebogi and J. Yorke, *Ergodic Theory Dyn. Syst.* **5**, 341 (1985).
 - [35] H. Faisst and B. Eckhardt, *Phys. Rev. E* **68**, 026215 (2003).
 - [36] S. S. P. Baker, M. Furlong and S. Harris, *Wildlife Biol.* **12**, 39 (2006).
 - [37] O. M. P. Rohani and M. Keeling, *Math. Med. Biol.* **21**, 63 (2004).
 - [38] J. Halley and P. Inchausti, *Fluc. Noise Lett.* **4**, R1 (2004).
 - [39] O. Miramontes and P. Rohani, *Physica D* **166**, 147 (2002).
 - [40] D. Thomson, *Proc. IEEE* **70**, 1055 (1982).
 - [41] N. Kasdin, *Proc. IEEE* **83**, 802 (1995).
 - [42] J. Hosking, *Biometrika* **68**, 165 (1981).
 - [43] M. Kennel and S. Isabelle, *Phys. Rev. A* **46**, 3111 (1992).